Structural, morphological, and optical properties of AlGaN/GaN heterostructures with AlN buffer and interlayer

S. Çörekçi, M. K. Öztürk, B. Akaoğlu, M. Çakmak,[a] and S. Özçelik
Department of Physics, Gazi University, 06500 Ankara, Turkey

E. Özbay
Nanotechnology Research Center, Department of Physics, and Department of Electrical and Electronics Engineering, Bilkent University, Bilkent, 06800 Ankara, Turkey

(Received 31 January 2007; accepted 30 April 2007; published online 18 June 2007)

$Al_xGa_{1-x}N/GaN$ ($x \sim 0.3$) heterostructures with and without a high-temperature (HT) AlN interlayer (IL) have been grown on sapphire (Al_2O_3) substrates and AlN buffer/Al_2O_3 templates by metal organic chemical vapor deposition. The effects of an AlN buffer layer (BL) grown on an Al_2O_3 substrate and an AlN IL grown under the AlGaN ternary layer (TL) on structural, morphological, and optical properties of the heterostructures have been investigated by high-resolution x-ray diffraction, spectroscopic ellipsometry, atomic force microscopy, and photoluminescence measurements. The AlN BL improves the crystal quality of the AlGaN TL. Further improvement is achieved by inserting an AlN IL between GaN BL and AlGaN TL. However, experimental results also show that a HT AlN IL leads to relatively rough surfaces on AlGaN TLs, and an AlN IL changes the strain in the AlGaN TL from tensile to compressive type. In addition, an AlN BL improves the top surface quality of heterostructures. © *2007 American Institute of Physics*.
[DOI: 10.1063/1.2747216]

I. INTRODUCTION

AlGaN/GaN heterostructures have been attracting much attention for nitride high-electron-mobility transistor (HEMT) applications.[1–6] Therefore, research on HEMTs has mainly focused on the growth of AlGaN/GaN heterostructures with high crystal quality. It is rather well known that III-V nitrides are generally grown on Al_2O_3 substrates due to their low cost, stability at high temperatures, and mature growth technology. However, their lattice parameters and thermal expansion coefficients are not well matched. The large lattice mismatch leads to high dislocation densities of 10^7-10^{11} cm^{-2} in the epilayer.[7–9] Therefore, AlGaN/GaN heterostructures with high *crystal quality* are typically grown for various buffer layers on the substrate. Recently, it has been reported that the crystal quality of GaN epitaxial films grown on an AlN buffer/Al_2O_3 template is considerably improved.[10,11]

On the other hand, the enhancement of *two-dimensional electron-gas (2DEG) density* and *mobility* in HEMTs has been more or less successful by different methods. For instance, an AlGaN ternary layer (TL) was doped with silicon in order to increase 2DEG density but this increase was rather limited.[5,6,12] In other studies, an increase of Al content in the AlGaN TL resulted in an increase in 2DEG density due to stronger spontaneous polarization and piezoelectric effects,[13–15] but electron mobility was reduced due to the enhancement of lattice stress, interface roughness, and alloy disorder scattering.[16–19] Apart from these methods, it has been found that the insertion of an AlN interlayer (IL) between an AlGaN TL and a GaN buffer layer (BL) (AlGaN/AlN/GaN) remarkably improves 2DEG density and electron mobility, due to the larger conduction band offset (ΔE_c) induced by the AlN IL and the decreased alloy disorder.[20–22] Although AlN BLs and AlN ILs have been widely employed in HEMTs based on AlGaN/GaN heterostructures, their effects on structural, morphological, and optical properties have not been completely clarified as of yet.

In the present study, we investigate the effects of an AlN BL on an Al_2O_3 substrate and an AlN IL between an AlGaN TL and a GaN BL on structural, morphological, and optical properties of AlGaN/GaN heterostructures. We found that AlN BL and AlN IL have a significant influence on the crystal quality, strain, interface, and surface properties of the heterostructures.

II. EXPERIMENT

Three samples were grown on a *c*-face Al_2O_3 substrate and AlN buffer/Al_2O_3 templates by low-pressure metal organic chemical vapor deposition (MOCVD). Hydrogen was used as the carrier gas and trimethylgallium (TMGa), trimethylaluminum (TMAl), and ammonia (NH_3) were used as source compounds. Prior to the epitaxial growth, Al_2O_3 substrates were annealed at 1100 °C for 10 min in order to remove surface contamination. As shown in Fig. 1, the AlGaN/AlN/GaN heterostructure grown on the Al_2O_3 substrate was labeled sample A. The AlGaN/AlN/GaN and AlGaN/GaN-heterostructures grown on AlN buffer/Al_2O_3 templates were labeled samples B and C. For sample A, a semi-insulating GaN was prepared by way of a two-step growth method with a 25-nm-thick low-temperature (LT) GaN nucleation deposited at 540 °C. The nucleation and annealing process were carefully calibrated to obtain highly resistive GaN. For samples B and C, first, a 15-nm-thick AlN nucleation layer

[a]Corresponding author; electronic mail: cakmak@gazi.edu.tr

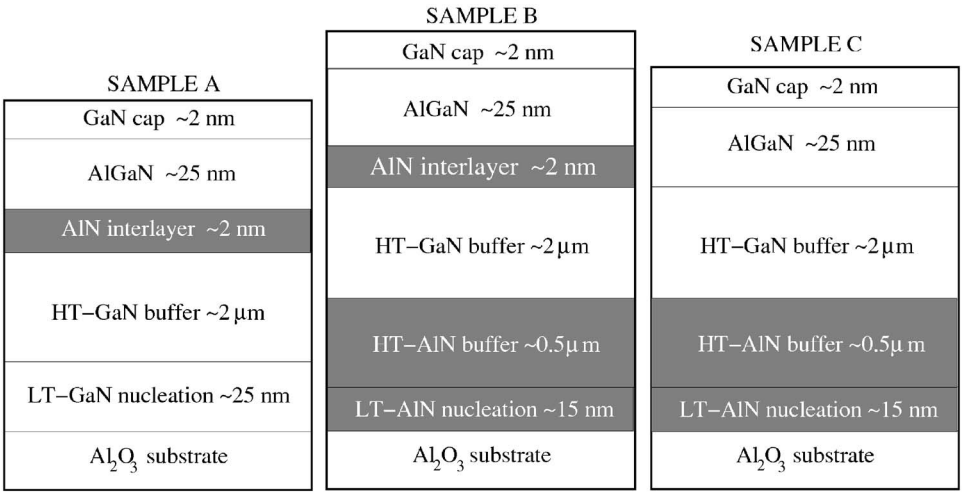

FIG. 1. Schematic structures of samples A, B, and C.

was deposited at 840 °C. Then, the reactor temperature was ramped to 1150 °C and a high-temperature (HT) AlN BL was grown, followed by a 2-min growth interruption in order to reach growth conditions for GaN. The GaN BL was grown at a reactor pressure of 200 mbar, a growth temperature of 1070 °C, and a growth rate of ~2 μm/h. Then, for samples A and B, the 2-nm-thick HT AlN IL was grown at a temperature of 1085 °C and a pressure of 50 mbar. Finally, for all of the samples, a 25-nm-thick AlGaN TL and a 2-nm-thick GaN cap layer growth were carried out at a temperature of 1085 °C and a pressure of 50 mbar, respectively.

The samples were characterized by high-resolution x-ray diffraction (HRXRD), x-ray reflectivity (XRR), spectroscopic ellipsometry (SE), atomic force microscopy (AFM), and photoluminescence (PL) measurements. The HRXRD measurements were performed by using a D8/Bruker diffractometer, equipped with a Cu source and a Ge(022) monochromator, which consists of a four-reflection channel-cut (220) oriented Ge crystal in the $(+n, -n, -n, +n)$ mode. The simulations of HRXRD and XRR scan data were performed with the commercial software LEPTOS 1.07 by using kinetic and dynamic methods. AFM (Omicron VT-STM/AFM) measurements were carried out at room temperature and atmosphere pressure. Ellipsometry measurements were performed in air at angles of incidence (AOIs) of 55°, 65°, and 75° with a spectroscopic phase modulated ellipsometer (Jobin Yvon-Horiba) in the spectral range between 1.5 and 4.7 eV. The system mainly consists of a light source (75 W xenon), an analyzer head (polarizing lens), a photoelastic modulator head including a polarizer, a monochromator, and a control unit. The arms holding the analyzer and modulator heads are mounted to a goniometry unit that enables the setting of AOIs in steps of 0.01°. The orientations of the analyzer and modulator are set to 45° and 0°, respectively. A 55 mW He-Cd laser (325 nm) is used as a light source in room temperature PL measurements.

III. RESULTS AND DISCUSSION

Figure 2 shows the x-ray diffraction (XRD) scans obtained for samples A, B, and C, in which the results confirm the nominal structures illustrated in Fig. 1. The high-resolution close-up view of the diffraction peaks with simulation results is shown in Fig. 3. The three main peaks are the (002) zeroth-order Bragg reflections from the GaN BL, AlGaN TL, and AlN BL. The peaks of GaN and AlGaN for samples A and B are relatively apparent, but not easily distinguishable for sample C as seen in Fig. 3. In addition, the full width at half maximum (FWHM) values, determined

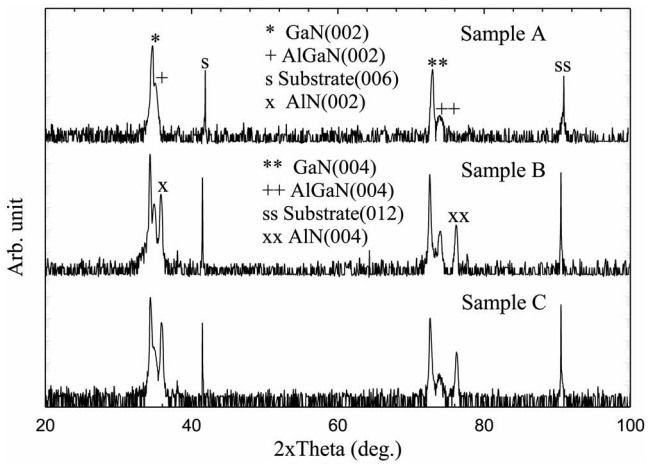

FIG. 2. X-ray reflections of samples A, B, and C.

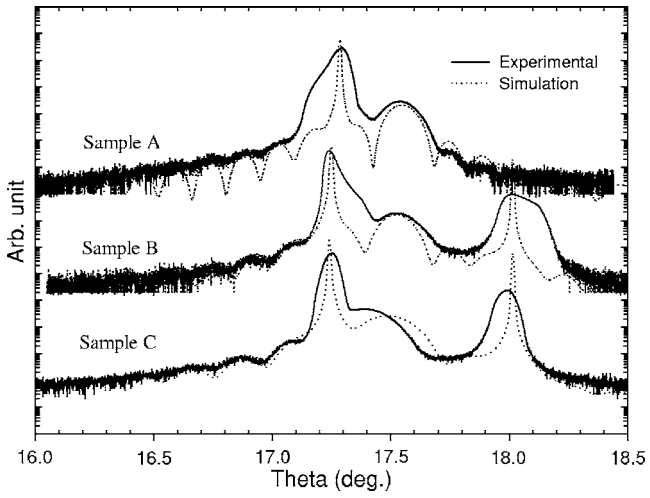

FIG. 3. High-resolution Bragg reflections near the (002) reflection of samples A, B, and C with simulation curves.

TABLE I. Simulation results obtained from HRXRD and XRR for samples A, B, and C.

	HRXRD						XRR					
	Al content ±0.5%			Strain/Relaxation			Thickness ±0.1 nm			Roughness ±0.1 nm		
Layers	A	B	C	A	B	C	A	B	C	A	B	C
GaN	–	–	–	0.016/–	0.015/–	0.016/–	2.19	2.30	2.53	0.58	0.50	0.32
AlGaN	31.02	29.00	30.90	0.040/0.060	0.040/0	−0.016/0.050	22.05	26.98	20.79	1.42	2.95	0.41
AlN	–	–	–	−0.051/0.102	−0.052/0	–	2.25	2.51	–	0.35	0.81	–
GaN	–	–	–	−/−	0.043/0.833	0.043/0.794	2028.20	1600.62	1838	3.73	1.39	0.72
AlN	–	–	–	–	−/−	−/−	–	504.82	715.42	–	1.39	0.10

from the x-ray rocking curves for the symmetric plane (0002) of AlGaN (GaN) layers in samples A, B, and C, are obtained as 437 (224), 333 (150), and 352 (191) arcsec. As the FWHM values of AlGaN and GaN layers in samples A and B are compared, it is clearly seen that the growth of the AlN BL improves the crystal quality of these layers. As the FWHM values of AlGaN and GaN layers in samples B and C are compared, the growth of the AlN IL is found to improve the crystal quality of these layers. In other words, these results show that an AlN BL improves the crystal quality of an AlGaN TL. Further improvement is achieved by inserting an AlN IL between the GaN BL and AlGaN TL. The Al content in the AlGaN TL and the strain and relaxation degrees throughout the whole structures were calculated from the simulations, and the results are tabulated in Table I. Our obtained Al contents for the samples were found to be in agreement with the nominal values ($x \sim 0.3$) within the error limits. Such an agreement is essential to compare the properties of the AlGaN TL, independent of the Al content. The strain in the AlGaN TL grown on GaN (in sample C) is tensile, because of the lattice mismatch between the AlGaN and GaN layers. However, AlGaN TLs grown on an AlN IL (in samples A and B) are compressively strained in parallel to the growth direction; the magnitude of this strain was found to be relatively higher in these samples in comparison to sample C. This compressive strain is due to the thermal mismatch between the AlGaN and AlN layers that comes out during the cooling down to room temperature of the grown structure. This observation shows that an AlN IL changes the strain in the AlGaN TL from the tensile to the compressive type, which is in agreement with the results in the literature.[23,24] Moreover, the relaxation degrees of the AlGaN TLs and AlN layers in all of the samples are nearly zero, whereas GaN BLs in samples B and C have a natural degree of relaxation.

Figure 4 shows the XRR curves for the samples in an angular interval of 0.2°–3.5°. Each sample exhibits weak periodical oscillations, which are commonly known as Kiessig fringes. The amplitudes of the fringes for samples B and C are observed to be higher due to the presence of the AlN BL. The frequency and amplitude of the oscillations are influenced by the interface roughness, thickness of the individual layers, and differences in the densities of these layers. In order to assess these points, XRR scans are needed in order to be fitted. In the fitting process, the strong contribution of the background, which also depends on the sample orientation, is subtracted from the data and a best fit is obtained for each sample. The obtained thickness and roughness values for the layers are presented in Table I. The roughness in the upper surfaces of GaN BLs indicates that the presence of an AlN BL improves the quality of these surfaces. This result is probably due to the reduction of dislocations propagating into GaN BL from the AlN BL. The degree of this improvement might be closely related to the thickness of the AlN BL, which is found to be larger (~715 nm) for the sample C.[25] On the contrary, the presence of the AlN ILs in samples A and B leads to relatively rough surfaces on AlGaN TLs in comparison to sample C. Recently, Jin *et al.*[23] investigated the effect of HT AlN IL on the structural properties of heterostrucutures without AlN buffer and found that heterostrucures with a HT AlN IL display high structural quality but with a rough surface, which is in agreement with our results. In their study, the poorer surface quality of AlGaN TLs grown on HT AlN IL was attributed to the high growth temperature (1040 °C) of HT AlN IL.[23] Within this framework, the high growth temperature (1085 °C) of HT AlN ILs for samples A and B probably leads to such an enhancement in the upper surface roughness of AlGaN TLs. However, the possibility of unintentional change in the growth conditions should not be excluded. For example, the control of the growth temperature of AlN ILs is rather critical, which might considerably change the flow rates during growth. Densities of AlGaN TLs for samples A, B, and C are 5.711, 6.088, and 5.206 g cm^{-2}, respectively. The strain and density values of AlGaN TLs in the samples with an IL are greater than those for a AlGaN TL without an IL.

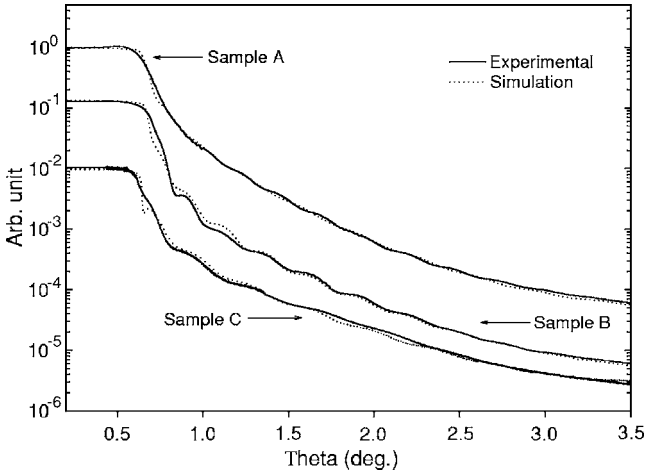

FIG. 4. Specular x-ray reflectivity of samples A, B, and C. Solid and dotted lines show the experimental data and fitted curves, respectively.

As was previously noted (see the Introduction), the main purpose for the insertion of an AlN IL between the GaN BL and AlGaN TL is to improve the 2DEG properties (2DEG density and mobility) in nitride HEMT structures. One of the most essential factors affecting 2DEG mobility is the interface scattering. Therefore, atomically abrupt and flat interfaces are rather important.[4] The eventual 2DEG mobilities in samples A and B are expected to be lower than that of sample C. The preliminary results on mobility measurements support this expectation and a detailed analysis of the electrical properties will be published elsewhere.

Figure 5 shows AFM images with a 5×5 μm^2 scan area obtained on the GaN cap layer surfaces of samples A, B, and C. Randomly oriented terrace steps suggest a step flow growth mode. While the step flow growth is beneficial, the defects on the surfaces are deleterious for device performance.[26] This growth mode creates a smooth surface morphology. The approximate step heights on samples A, B, and C are determined as 0.27, 0.24, and 0.24 nm, respectively. These measured values are rather close to the thickness of the monolayer of (002) GaN.

Most of the terrace steps shown on the GaN surface are pinned, generally appearing as dark spots in the AFM images. The pinned steps should be associated with the screw threading dislocations (TDs), since a pinned step must be formed when a TD with a screw component intersects a free crystal surface and causes a surface displacement normal to the surface.[27] The screw-type dislocation densities of samples A, B, and C are estimated as 2×10^9, 2.5×10^8, and 5.2×10^8 cm^{-2} $(\pm0.2\times10^8)$, respectively. The dislocation density of sample B is approximately one order of magnitude lower than that of sample A. The root mean square (rms) roughness values for samples A, B, and C are obtained as 0.70, 0.27, and 0.30 nm, respectively. Table II summarizes the screw-type TD dislocation densities and rms roughness on GaN surfaces for samples A, B, and C. The surface roughness is closely related to the lateral step sizes on the GaN surfaces. Laterally larger steps, appearing on the surface, suggest lower roughness on the surface. As seen in Fig. 5, the steps on the surfaces of samples B and C grown by using an AlN BL are larger than those on the surface of sample A. These direct observations from the AFM images are in agreement with the measured surface rms roughness values. In other words, lateral step flow growth and surface smoothing seem to be occurring in harmony. The dislocation densities and rms roughness values for samples B and C grown on AlN buffer/Al_2O_3 templates are found to be lower in comparison to those for sample A grown on Al_2O_3 substrate. This is in agreement with recently reported results.[4,10] Additionally, the dislocation densities and rms roughness values of samples B and C grown on an AlN buffer/Al_2O_3 template are found to be similar to each other. The AFM results clearly indicate that the AlN BL improves the top surface quality. XRR results show that, among the samples grown on an AlN buffer/Al_2O_3 template, the top surface roughness of sample B is found to be high due to the HT AlN IL. However, this negative effect is not observed in AFM results, which might be due to the relatively small probed surface area in AFM measurements.

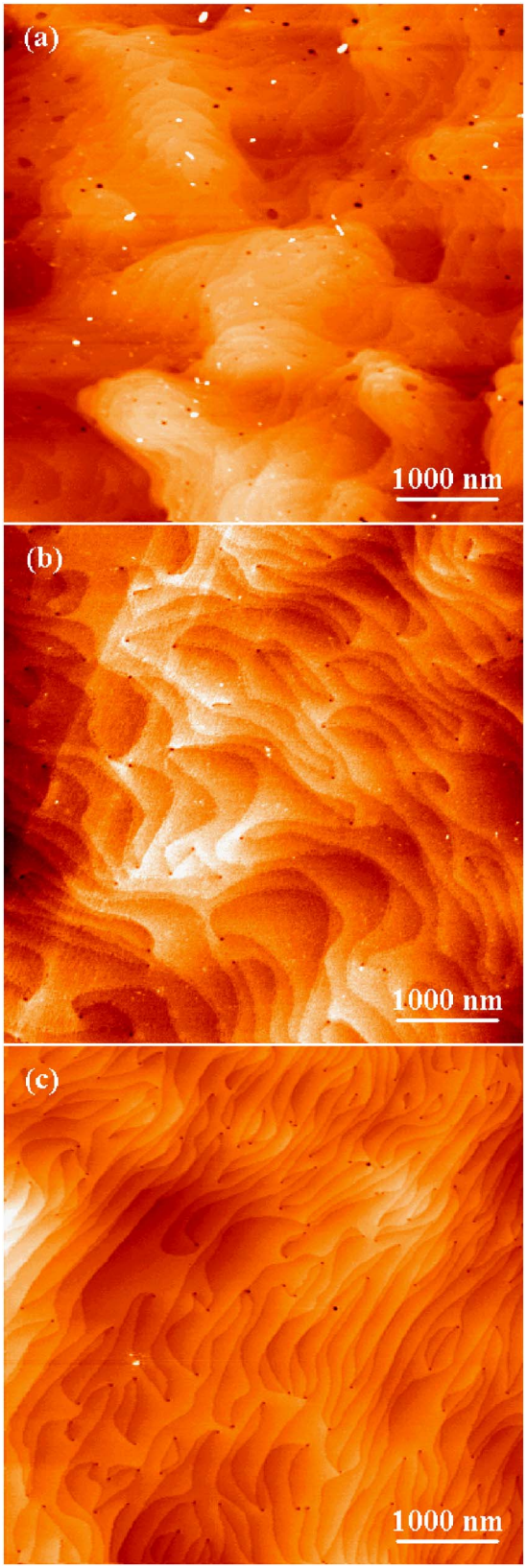

FIG. 5. AFM images with a 5×5 μm^2 scan area of samples (a) A, (b) B, and (c) C.

Ellipsometry is a nondestructive and highly sensitive method that is based on the measurement of the change of polarization of light upon reflection (or transmission) from surfaces or interfaces.[28] The ratio of complex reflection co-

TABLE II. The dislocation densities and rms roughness on GaN surfaces for samples A, B, and C.

Samples	Dislocation density ($\pm 0.20 \times 10^8$ cm^{-2})	rms roughness (nm)
Sample A	2.0×10^9	0.70
Sample B	2.5×10^8	0.27
Sample C	5.2×10^8	0.30

efficients of incident light polarized parallel (r_p) and perpendicular (r_s) to the plane of incidence is conventionally expressed in terms of ellipsometric angles Ψ and Δ as $\rho = r_p/r_s = \tan(\Psi)e^{i\Delta}$. The real ($\langle\varepsilon_1\rangle$) and imaginary parts ($\langle\varepsilon_2\rangle$) of the pseudodielectric functions ($\langle\varepsilon\rangle$) of the samples, shown in Figs. 6(a) and 6(b) only for an AOI of 65°, were determined by assuming a two-phase (one-interface) optical model according to

$$\langle\varepsilon\rangle = \langle\varepsilon_1\rangle + i\langle\varepsilon_2\rangle = \varepsilon_a \sin^2\varphi_0\left[1 + \tan^2\varphi_0\left(\frac{1 - \tan\Psi e^{i\Delta}}{1 + \tan\Psi e^{i\Delta}}\right)^2\right]. \quad (1)$$

The measurement results of the AOIs of 55° and 75° are not shown in Figs. 6(a) and 6(b) for clarity. Interference oscillations below the fundamental band gap of GaN at 3.43 eV are due to multiple reflections and transmissions within the entire epitaxial multilayer structure, and their frequencies are mainly related to the thicknesses of the buffer layers. Beyond this energy, a weak interference pattern is still observed especially for sample B due to the AlN BL. The modulation of the fringes originates from the uniaxial anisotropic nature of the backside-polished Al_2O_3 substrate with a thickness of 330 μm. The spectra of both $\langle\varepsilon_1\rangle$ and $\langle\varepsilon_2\rangle$ display a pronounced excitonic structure at the band gap energy of the AlGaN TL. The Al content of the AlGaN can be estimated from the positions of these prominent resonance peaks appearing in the $\langle\varepsilon_1\rangle$ spectra. Small differences in the thicknesses of AlGaN TLs that might be present in samples A, B, and C, may influence the positions of the peaks, but this effect is negligibly small in comparison to the effect of Al content.[29] Substituting the observed band gaps of AlGaN in the empirical relations provided in Refs. 20–33, the Al contents of samples A, B, and C were estimated as 0.28, 0.30, and 0.25 (±0.03), respectively. The decrease in atomic density is expected to lead to a decrease in $\langle\varepsilon_2\rangle$, which is, by definition, related to dipole moment per volume. In this framework, the lower values of $\langle\varepsilon_2\rangle$ in the energy range where the penetration depth of light is of the order of the roughness scale suggest an enhancement of the microscopic surface roughness.[34] As seen in Fig. 6(b), the $\langle\varepsilon_2\rangle$ values for samples B and C appear considerably higher than for sample A beyond approx. 4 eV. Therefore, the surface quality of sample A is found to be relatively poorer, which is in agreement with the AFM and XRR results. The normalized broadening (Γ) of the excitonic feature of the samples, seen in Fig. 6(c), is determined and plotted as a function of AOI as shown in Fig. 6(c). These broadening parameters are not full width at half maximum values; instead, they represent the energy broadening between 0.15 eV above and 0.15 eV below the corresponding energy of the peak maximum. These broadening parameters are normalized with respect to the broadening for sample B. The areas of the surfaces probed by the beam of light in the ellipsometry measurements at AOIs 55°, 65°, and 75° are 1.4, 1.9, and 3.0 mm^2, respectively. The normalized Γ values for the samples generally exhibit increasing tendencies as AOI increases, and this be-

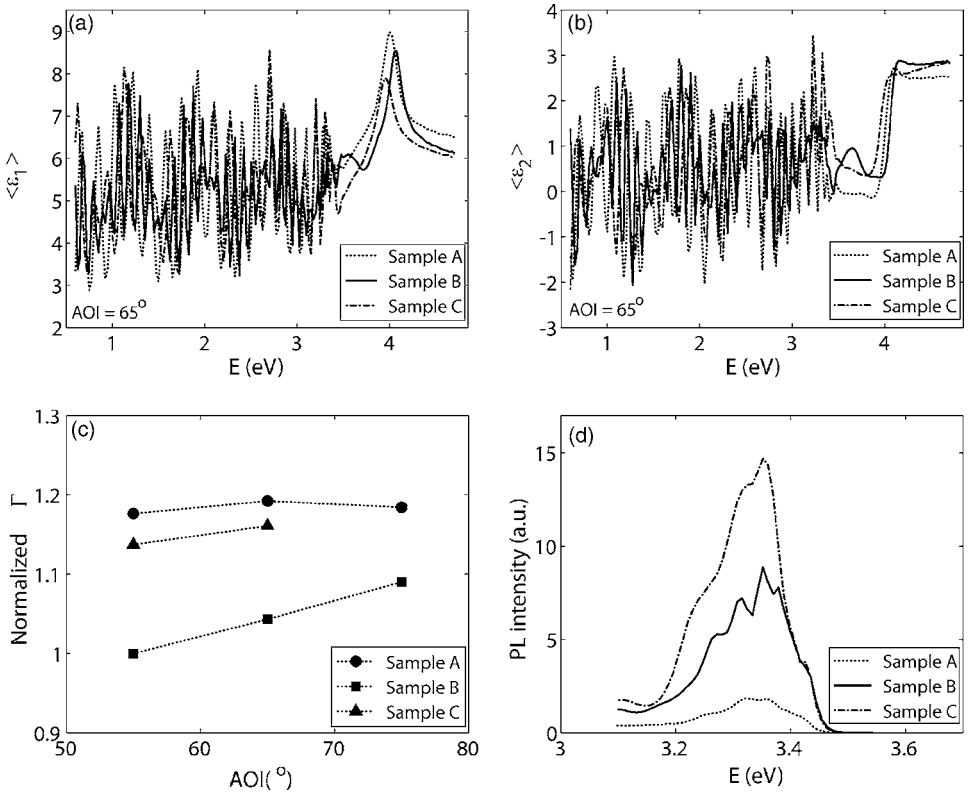

FIG. 6. (a) Real and (b) imaginary parts of the pseudodielectric function of the samples obtained from ellipsometry measurements at an AOI of 65°; (c) normalized broadening (Γ) of the excitonic peaks appearing in $\langle\varepsilon_1\rangle$ spectra that are normalized with the broadening parameter that was obtained for sample B at an AOI of 55°; (d) photoluminescence spectra of all the samples measured at room temperature.

havior is more evident for sample B. These results suggest that the degree of lateral nonuniformities increases as the probed surface area becomes larger. Sample A with the AlN IL has the largest broadening and sample C has a larger broadening than sample B with the AlN IL. These results are in agreement with the FWHM values obtained from the HRXRD measurements and show that both AlN IL and AlN BL improve the crystal quality of the AlGaN TL.

The photoluminescence spectra for the samples, measured at room temperature, are shown in Fig. 6(d) and a strong emission at ~3.37 eV is observed. The spectra show that PL intensities for samples B and C that are grown with a AlN BL are higher than for sample A. This remarkable result suggests that the AlN BL considerably reduces the amount of propagation of the dislocations into the GaN BL, which is in agreement with the upper surface roughness of the GaN BLs obtained from the XRR measurements. It has been recently shown that photoluminescence intensity increases as the thickness of GaN increases up to 800 nm for a multiple quantum well structure.[35] In light of this information, the reason for the higher PL intensity for sample C compared to sample B might be the larger thickness of the AlN BL that is present in sample C. In addition, the interface roughness value for sample C obtained from x-ray analysis is lower. This result also supports the enhancement in the PL intensity.

IV. CONCLUSION

We have investigated the effect of an AlN IL and AlN BL on AlGaN/GaN heterostructures grown on Al_2O_3 substrates by MOCVD. The AlN BL improves the crystal quality of AlGaN TL, and further improvement is achieved by inserting an AlN IL between the GaN BL and AlGaN TL. However, the HRXRD results show that a high-temperature AlN IL leads to relatively rough surfaces on AlGaN TLs and the AlN IL changes the strain in the AlGaN TL from the tensile to compressive type. The AFM results show that the AlN buffer/Al_2O_3 template reduces the screw-type dislocation density and rms roughness of the top surface. The broadening (Γ) of the excitonic feature at the band gap energy of the AlGaN TL is found to be minimum from the SE measurements for the sample grown with AlN IL and AlN BL. Furthermore, the PL spectra of the samples similarly suggest enhanced crystal quality in the samples with an AlN BL, but this effect is larger for sample C, which includes a thicker AlN BL. This observation clearly demonstrates the role of the AlN BL, which in turn suppresses the propagation of dislocations into GaN BL.

ACKNOWLEDGMENTS

This work was supported by the Turkish State Planning Organization (Project No. 2001K120590). This work is supported by TUBITAK under Project Nos. 104E090, 105E066, and 105A005. One of the authors (E.O.) also acknowledges partial support from the Turkish Academy of Sciences.

[1] S. Arulkumaran, T. Egawa, H. Ishikawa, and T. Jimbo, Appl. Phys. Lett. **80**, 2186 (2002).
[2] H. Xing, S. Keller, Y.-F. Wu, L. McCarthy, I. P. Smorchkova, D. Buttari, R. Coffie, D. S. Green, G. Parish, S. Heikman, L. Shen, N. Zhang, J. J. Xu, B. P. Keller, S. P. DenBaars, and U. K. Mishra, J. Phys.: Condens. Matter **13**, 7139 (2001).
[3] M. Miyoshi, H. Ishikawa, T. Egawa, K. Asai, M. Mouri, T. Shibita, M. Tanaka, and O. Oda, Appl. Phys. Lett. **85**, 1710 (2004).
[4] M. Miyoshi, T. Egawa, H. Ishikawa, K.-I. Asai, T. Shibita, M. Tanaka, and O. Oda, J. Appl. Phys. **98**, 063713 (2005).
[5] C. Wang, X. Wang, G. Hu, J. Wang, J. Li, and Z. Wang, Appl. Surf. Sci. **253**, 762 (2006).
[6] C. Wang, X. Wang, G. Hu, J. Wang, H. Xiao, and J. Li, J. Cryst. Growth **289**, 415 (2006).
[7] N. G. Weimann and L. F. Eastman, J. Appl. Phys. **83**, 3656 (1998).
[8] D. Kapolnek, X. H. Wu, B. Heying, S. Keller, B. P. Keller, U. K. Mishra, S. P. DenBaars, and J. S. Speck, Appl. Phys. Lett. **67**, 1541 (1995).
[9] S. D. Lester, F. A. Ponce, M. G. Craford, and D. A. Steigerwald, Appl. Phys. Lett. **66**, 1249 (1995).
[10] M. Miyoshi, A. Imanishi, T. Egawa, H. Ishikawa, K. Asai, T. Shibita, M. Tanaka, and O. Oda, Jpn. J. Appl. Phys., Part 1 **44**, 6490 (2005).
[11] H. B. Yu, M. K. Ozturk, S. Ozcelik, and E. Ozbay, J. Cryst. Growth **293**, 273 (2006).
[12] O. Ambacher, B. Foutz, J. Smart, J. R. Shealy, N. G. Weimann, K. Chu, M. Murphy, A. J. Sierakowski, W. J. Schaff, and L. F. Eastman, J. Appl. Phys. **87**, 334 (2000).
[13] S. Arulkumaran, T. Egawa, H. Ishikawa, and T. Jimbo, J. Vac. Sci. Technol. B **21**, 888 (2003).
[14] C. Wang, X. Wang, G. Hu, J. Wang, and J. Li, Phys. Status Solidi C **3**, 486 (2006).
[15] G. Parish, S. Keller, S. P. Denbaars, and U. K. Mishra, J. Electron. Mater. **29**, 15 (2000).
[16] S. Keller, G. Parish, P. T. Fini, S. Heikman, C.-H. Chen, N. Zhang, S. P. DenBaars, U. K. Mishra, and Y.-F. Yu, J. Appl. Phys. **86**, 5850 (1999).
[17] I. P. Smorchkova, C. R. Elsass, J. P. Ibbetson, R. Vetury, B. Heying, P. Fini, E. Haus, S. P. DenBaars, J. S. Speck, and U. K. Mishra, J. Appl. Phys. **86**, 4520 (1999).
[18] O. Ambacher, J. Smart, J. R. Shealy, N. G. Weimann, K. Chu, M. Murphy, W. J. Schaff, L. F. Eastman, R. Dimitrov, L. Wittmer, M. Stutzmann, W. Rieger, and J. Hilsenbeck, J. Appl. Phys. **85**, 3222 (1999).
[19] J. P. Ibbetson, P. T. Fini, K. D. Ness, S. P. DenBaars, J. S. Speck, and U. K. Mishra, Appl. Phys. Lett. **77**, 250 (2000).
[20] L. Hsu and W. Walukiewicz, J. Appl. Phys. **89**, 1783 (2001).
[21] I. P. Smorchkova, L. Chen, T. Mates, L. Shen, S. Heikman, B. Moran, S. Keller, S. P. DenBaars, J. S. Speck, and U. K. Mishra, J. Appl. Phys. **90**, 5196 (2001).
[22] L. Shen, S. Heikman, B. Moran, R. Coffie, N.-Q. Zhang, D. Buttari, I. P. Smorckhova, S. Keller, S. P. DenBaars, and U. K. Mishra, IEEE Electron Device Lett. **22**, 457 (2001).
[23] R. Q. Jin, J. P. Liu, J. C. Zhang, and H. Yang, J. Cryst. Growth **268**, 35 (2004).
[24] Z. X. Qin, H. J. Luo, Z. Z. Chen, Y. Lu, T. J. Yu, Z. J. Yang, and G. Y. Zhang, J. Mater. Sci. **42**, 228 (2007).
[25] K. Jeganathan, T. Ide, M. Shimizu, and H. Okumura, J. Appl. Phys. **93**, 2047 (2003).
[26] A. Torabi, P. Ericson, E. J. Yarranton, and W. E. Hooke, J. Vac. Sci. Technol. B **20**, 1234 (2002).
[27] F. C. Frank, Discuss. Faraday Soc. **5**, 67 (1949).
[28] D. E. Aspnes, in *Optical Properties of Solids: New Developments*, edited by B. O. Seraphin (North Holland, Amsterdam, 1976), p. 799.
[29] J. Wagner, H. Obloh, M. Kunzer, M. Maier, K. Kohler, and B. Johs, J. Appl. Phys. **89**, 2779 (2001).
[30] M. Baeumler, S. Muller, K. Kohler, and J. Wagner, Phys. Status Solidi A **202**, 665 (2005).
[31] F. Yun, M. A. Reshchikov, L. He, T. King, H. Morkoç, S. W. Novak, and L. Wei, J. Appl. Phys. **92**, 4837 (2002).
[32] K. B. Nam, M. L. Nakarmi, J. Y. Lin, and H. X. Jianga, Appl. Phys. Lett. **86**, 222108 (2005).
[33] C. Buchheim, R. Goldhahn, M. Rakel, C. Cobet, N. Esser, U. Rossow, D. Fuhrmann, and A. Hangleiter, Phys. Status Solidi B **242**, 2610 (2005).
[34] D. E. Aspnes, Thin Solid Films **89**, 249 (1982).
[35] J. Bai, T. Wang, P. Comming, P. J. Parbrook, J. P. R. David, and A. G. Cullis, J. Appl. Phys. **99**, 023513 (2006).